EVS24
Stavanger, Norway, May 13 - 16, 2009

CONTROLLED SERIES CAPACITOR CONVERTERS APPLIED IN GENERATOR-SETS FOR SHEV's

Volker Pickert, Dimitrios Kalpaktsoglou, Ahmed Al-Busaidi
Newcastle University, School of Electrical, Electronic and Computer Engineering,
Newcastle upon Tyne, NE17RU, UK, Email: volker.pickert@ncl.ac.uk

Abstract

This paper compares controlled series capacitor (CSC) converters applied to generator-sets used in series hybrid electric vehicles (SHEV). The operation of each circuit is discussed and simulated using Matlab/Simulink. It is concluded that CSC converters can improve the power factor (PF) of the generator-set.

Key words: CSC, SHEV, PF.

1 Introduction

An SHEV has its wheels driven by an electric motor powered by a battery with an engine plant that cranks a generator unit to provide electric power to the battery and if necessary to the electric motor. One of the major components of a SHEV is the generator unit. Generally, the generator unit consist of a 3-phase machine and a 3-phase rectifier circuit. There are four common rectifier circuits in SHEVs: uncontrolled full-bridge diode rectifier, controlled full-bridge Thyristor rectifier, uncontrolled full-bridge diode rectifier with dc/dc boost converter and PWM voltage-source current controlled rectifier. In [1] it was concluded that none of the rectifier circuits provides high PF with high output voltage in order to increase the overall efficiency of the power drive train of SHEVs. This is, because the inductance of the electric generator and the current commutation effect in the rectifier are reducing the PF of the generator-set.

One way to compensate the impact of the machine inductance is by adding a capacitor in series to the generator. Any inductive reactance can be eliminated when the inductive reactance X_L is equal to the capacitive reactance Xc, the system is at its resonant point, and PF becomes unity. Converters that make use of this approach are called controlled series capacitor (CSC) converters. This paper applies CSC converters to an uncontrolled full-bridge diode rectifier in order to assess this technology.

2 Controlled Series Capacitor (CSC) Converters

CSCs are not new topologies. They have been used in power transmission lines to improve the PF. So far, CSCs have never been applied to SHEVs, where the supply frequency is high and not fixed. This paper describes, for the first time, the benefits and drawbacks of using CSCs in SHEVs. Three different CSCs have been compared, using MATLAB/SIMULINK simulation, in terms of power factor, output voltage, total current harmonic distortion (%THD), and power losses. A 50kW three-phase electric generator (back EMF 325V, Ls=1.407mH, Rs=0.06Ω) was simulated to feed the rectifier circuit. CSCs consists of a variable capacitor placed between the generator and the uncontrolled full-bridge diode rectifier. The capacitor's value varies with respect to the electric frequency, in order to match the inductance of the generator. Therefore, any inductive reactance can be eliminated and the PF becomes unity.

CSCs operate at much lower switching frequency promising a reduction in switching losses, without PF degradation. The three investigated CSC circuits are called: thyristor-switched series capacitor (TSSC), switched variable capacitor (SVC), and forced commutation controlled series capacitor (FCSC). In the following figures the three investigated CSC circuits are illustrated and their principles of operation are presented. For each circuit a description of controlling the PF in order to maximize the power factor is explained.

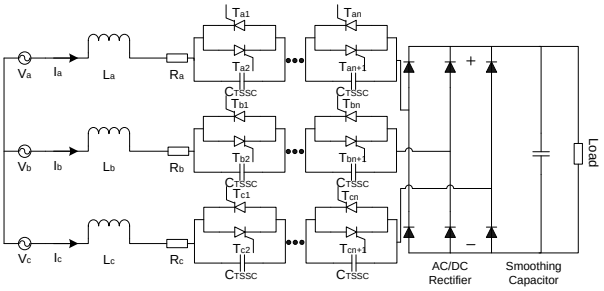

Figure 1: Thyristor-Switched Series Capacitor (TSSC)

The TSSC circuit, shown in Figure 1, consists of a number of capacitors in series, each shunted by a switch, composed of two anti-parallel thyristors [2]. All capacitors have the same value C_{TSSC}.

The battery and the electric drive of the SHEV power drive train is shown as a capacitor and a resistive load for simplicity. The machine is represented by the back EMF V, inductance L and resistance R.

The overall capacitance is controlled by conducting or blocking each of the thyristor pairs. If a thyristor pair conducts, the capacitor C_{TSSC} is short circuited. If a thyristor pair is open, the value C_{TSSC} is added to the total capacitance C_T. The total capacitance of the circuit is given by:

$$C_T = C_{TSSC} / m \qquad (1)$$

where m is the number of active capacitors. If all capacitors are bypassed the equivalent capacitance becomes C_T = 0 F. In order to correct the PF, X_C should be equal to the reactance X_L:

$$X_C = X_L \Rightarrow 1/\omega C_T = \omega L \Rightarrow C_T = 1/\omega^2 L \qquad (2)$$

The desired number of active capacitors for unity PF for every frequency can be calculated using equations (1) and (2)

$$C_{TSSC}/m = 1/\omega^2 L \Rightarrow m = C_{TSSC}\omega^2 L \qquad (3)$$

Since C_{TSSC} and L are fixed, m is directly related to the electric frequency f.

All the thyristors are commutated "naturally" and they turn off when the current crosses zero. At this time a capacitor can be inserted into the line as shown in Figure 2.

Once the capacitor is in line, it will be charged to its maximum value, during the full half-cycle of the line current and discharged from its maximum to zero during the negative line current cycle [2,3].

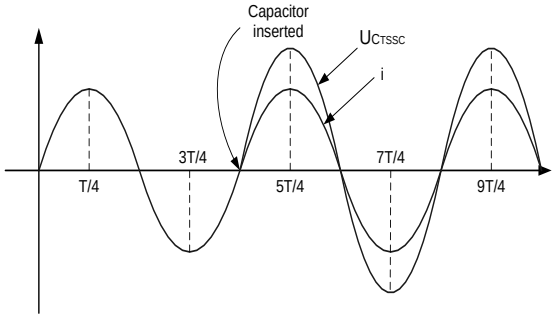

Figure 2: Capacitor insertion at zero current voltage

The SVC rectifier circuit consists of two parallel capacitors, C_1 and C_2, which are connected with two switches, S_1 and S_2, as shown in Figure 3.

The values of capacitors C_1 and C_2 have been chosen carefully to match the inductive reactance at low, and high frequencies. Therefore, capacitor C_1 will attempt to hit the resonant point at high frequencies, while capacitor C_2 was chosen for low frequencies. The two switches alternate in their switching status and the average capacitance C_{av} becomes a function of the duty factor [4].

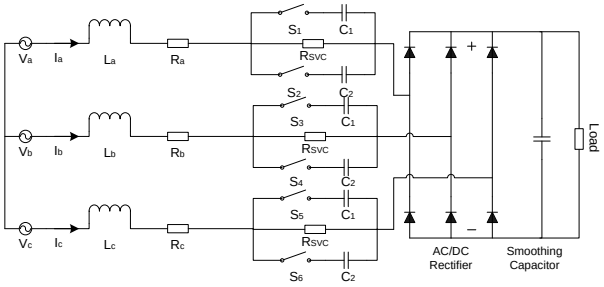

Figure 3: Switched Variable Capacitor (SVC)

In order to alternate the switching status PWM technique is used. This allows the change of the average capacitance. When the frequency is low, the inductive reactance becomes minimum and the PWM controller allows the current to pass through C_2 only. When the frequency is high, the inductive reactance becomes a maximum, and the capacitor C_2 is inactive while C_1 is inserted. For the frequencies in between, both capacitors are switched. Before one switch turns on the other must first turn off allowing continuity of current flow. For that reason the resistor R_{SVC} is integrated. The simulation used C_1=1.689mF and C_2=0.188mF.

The FCSC is shown in Figure 4 and it consists of a capacitor and a pair of switches, such as IGBTs for example, each anti-parallel connected [2].

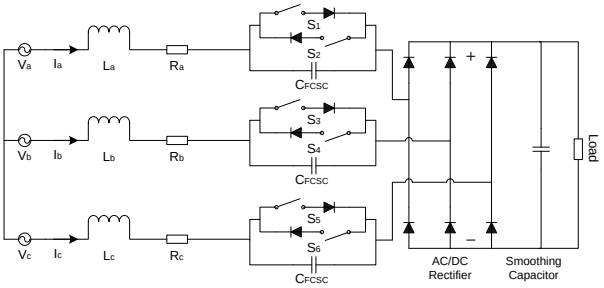

Figure. 4: Forced Commutation Controlled Series Capacitor (FCSC)

The principal target in this case is the same as in the last case. The capacitive reactance X_C can vary from $X_C = 0$ to $X_C = 1/\omega C$ in order to match any inductive reactance. When the IGBT switches S_1 and S_2 are closed, the capacitor bank is short circuited. When the switches are open the current flows through the capacitor C_{FCSC}. Therefore, the capacitor voltage can be controlled by closing and opening the switches each half-cycle. The series reactance can be expressed as:

$$X_{C(\gamma)} = \frac{V_C}{I} = \frac{1}{\omega C}\left(1 - (2/\pi)\gamma - (1/\pi)\sin 2\gamma\right) \quad (4)$$

where γ is the delay angle [2].

In Figure 5, the inductive reactance for frequencies up to 350 Hz is shown by the bold line. The thin curved lines represent the capacitive reactance for various delay angles γ over frequencies up to 350 Hz.

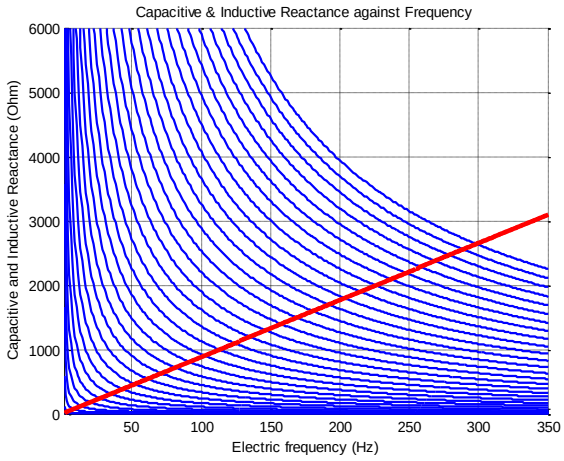

Figure 5: Capacitive and Inductive reactance against electric frequency

By choosing the appropriate delay angle γ, the system operates at its resonant point and the PF become unity.

3 Power factor calculation

The PF is an indicator of useful power that can be transferred from the source to the load. With a PF of 1 (PF=1) all of the real power available in an electric machine will be delivered to the output of the generator-set allowing maximum utilization of the machine. A high PF means also low line harmonics between the machine and the rectifier circuit.

The PF determines the ratio of the real power (P) to the complex power (S) as expressed in equation (5)

$$PF = \frac{Real\ \ Power}{Complex\ \ Power} = \frac{P}{S} = \frac{\frac{1}{T}\int_0^T vidt}{VI} \quad (5)$$

where v and i represent the Fourier Series

$$v = \sum_{n=0}^{\infty} \sqrt{2} V_n \sin\left(n\omega t + \alpha_{vn}\right)$$
$$i = \sum_{n=0}^{\infty} \sqrt{2} I_n \sin\left(n\omega t + \alpha_{in}\right) \quad (6)$$

and V and I represent the RMS values

$$V = \sqrt{\frac{1}{T}\int_0^T v^2 dt}$$
$$I = \sqrt{\frac{1}{T}\int_0^T i^2 dt} \quad (7)$$

In (6) α_{vn} and α_{in} are the phase delays for voltage and current respectively. Equation (5) becomes complex when (6) and (7) are used. In simulations, however, the back EMF can be simulated pure sinusoidal. In this case the PF can be calculated as follows:

$$PF = \frac{Real\ \ Power}{Complex\ \ Power} = \frac{P}{S} = \frac{V_1 I_1 \cos\left(\alpha_{v1} - \alpha_{i1}\right)}{VI} = \frac{I_1}{I}\cos(\alpha) \quad (8)$$

PF has become a function of the RMS current I, the RMS current of the first harmonic I_1 and the phase delay α between the voltage and the first harmonic of the current. Equation (8) shows that large distortions in the current waveform will result in a small $\frac{Is1}{Is}$ ratio and hence a low PF.

It is important to address that equation (8) should not be used when PF is calculated based on measurements. In real applications the back EMF is not pure sinusoidal and (8) becomes invalid. When

calculating the PF from real measured data equations (5), (6) and (7) must be applied.

4 Results and Discussions

All three circuits have been analysed and compared by simulation. Each circuit was tested at different engine speeds. The following results are shown for an engine speed of 3.000rpm. However, the statements given below will remain regardless the engine speed.

Figure 6 shows the comparison of the PF from all three CSCs compared to the uncontrolled full-bridge diode rectifier, for various load resistances (load currents). All CSCs achieve nearly unity PF, while the uncontrolled full diode bridge rectifier results in a very poor performance under all load conditions.

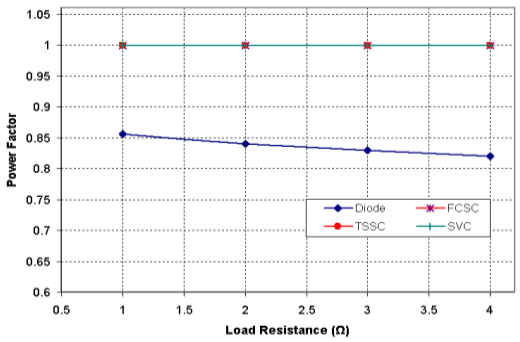

Figure. 6: Comparison of PF over load resistances (load currents) at an engine speed of 3.000rpm

The output voltage of the generator-set is shown in Figure. 7. The TSSC clearly shows the best performance (assuming the generator operates at constant speed) over the full load range. The output voltage of the TSSC is highest when the load current is low (high load resistance). The conventional uncontrolled full diode bridge rectifier circuit has a significant voltage drop which is caused by two effects: 1) absent of PF correction 2) a large current commutation time. Current commutation is a function of the size of the machine inductance. In CSC's this commutation is minimised. The process of current commutation and the impact on output voltage of rectifier circuits are discussed in more details in [1].

From figures 6 & 7 one can conclude that CSC's can improve PF and output voltage compared to the uncontrolled full-bridge diode rectifier. Out of all three CSC's investigated the TSSC gives the best performance as it demonstrates highest PF and highest output voltage.

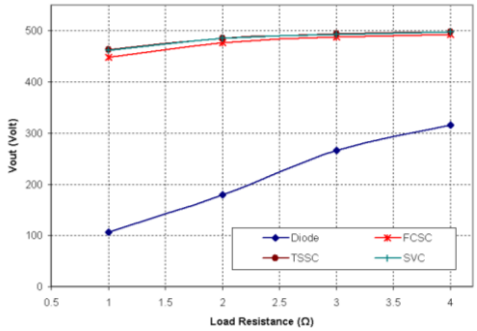

Figure .7 Comparison of the output voltage over load resistances (load currents) at an engine speed of 3.000rpm

Table 1 shows the simulation results of the three CSC and the uncontrolled full diode bridge rectifier circuit. Data collected are the RMS value of the first current harmonic, the total current harmonic distortion, the output voltage and the total losses for an engine speed at 3.000rpm.

Table 1: Simulation results for an engine speed of 3.000rpm

	Rload (Ω)	I1rms (A)	%THD	Output voltage (V)	Losses (kW)
FCSC	4	89.87	4.355	493	0.67
	3	117.5	3.343	487.5	1.13
	2	170	2.331	476.8	2.38
	1	308.9	1.306	448	7.82
SVC	Rload (Ω)	I1rms (A)	%THD	Output voltage (V)	Losses (kW)
	4	92.53	4.075	497.9	0.09
	3	122.2	3.059	493.9	0.15
	2	180.1	2.039	485.9	0.30
	1	343.2	1.011	463.5	1.03
TSSC	Rload (Ω)	I1rms (A)	%THD	Output voltage (V)	Losses (kW)
	4	88.44	5.43	497.6	0.07
	3	123.1	3.49	493.4	0.11
	2	182.3	2.19	485.3	0.21
	1	342.5	1.09	462.6	0.70
Diode Bridge	Rload (Ω)	I1rms (A)	%THD	Output voltage (V)	Losses (kW)
	4	58.8	3.97	316	0.07
	3	65.8	3	266.2	0.04
	2	73.0	2	179	0.02
	1	78.7	1	106.4	0.02

Table 1 shows that the additional components in CSC circuits add switching losses and conduction losses. These losses can become higher compared to the losses generated by the uncontrolled full bridge diode rectifier circuit. Generally, the losses become higher at high load current conditions (low load resistance).

5 Conclusion

The performance of rectifier circuits in generator-sets for SHEVs can be improved by adding CSC circuitries. CSC will eliminate the effect of PF degradation caused by the inductance of the machine under all speed conditions. A high PF leads to a better utilization of the machine which allows the downsizing of the machine. However, losses added by the additional components may offset the benefit of CSC circuits.

Acknowledgments

The authors would like to thank the Engineering and Physical Sciences Research Council for their support of this research.

References

[1] A. Al-Busaidi, V. Pickert, “Comparative study of rectifier circuits for series hybrid electric vehicles”, presented at Hybrid & Eco-friendly Vehicle Conference 2008 (HEVC08), Warwick, UK, 2008.

[2] M. H. Rashid, *Power Electronics: Circuits, Devices and Applications*, 3rd ed. Upper Saddle River, N.J.: Prentice Hall, 2004.

[3] N. G. Hingorani and L. Gyugyi, Understanding FACTS: concepts and technology of flexible AC transmission systems. New York: IEEE Press, 2000.

[4] T. Miyasaka, K. Yamazaki, J. Tsuchiya, T. Shimizu, G. Kimura, and M. Shioya, "Improved operating characteristics of linear pulse motor using resonant current," presented at Proceedings of the 19th International Conference on Industrial Electronics, Control and Instrumentation, Nov 15-18 1993, Maui, Hawaii, USA, 1993.

Authors

Volker Pickert received his Dipl.-Ing. in Electrical and Electronic Engineering from the RWTH Aachen, Germany and the University of Cambridge, UK in 1994. He received his PhD from Newcastle University in 1997. In 1998 he started at Semikron International as application engineer and moved later to Volkswagen where he became group leader for electric drives for electric-, hybrid- and fuel cell vehicles. Since October 2003 he is a Senior Lecturer at Newcastle University. His research interests are power electronics for automotive applications, thermal management, fault tolerant converters and nonlinear controllers.

Ahmed Al-Busaidi is a PhD student within the Power Electronics, Drives and Machines Group at Newcastle University. He received his MSc from Newcastle University in 2005 and his BENG from Sultan Qaboos University, Sultanate of Oman in 2000. His research interests are power electronics for automotive applications, drives and power generation.

Dimitrios Kalpaktsoglou graduated in 2003 from the University of Lincoln, with a BEng (Hons) in Engineering (Mechanical & Electrical). He studied his Master Degree (MSc) at Newcastle University on Electrical Power. In 2004 he started his PhD at Newcastle University. His interests are power electronics and renewable energy.